

Effect of quantum resonances on local temperatures of nonequilibrium open systems

Xiangzhong Zeng,¹ Lyuzhou Ye,¹ Daochi Zhang,¹ Rui-Xue Xu,¹ Xiao Zheng,^{2,*} and Massimiliano Di Ventra^{3,†}

¹*Hefei National Laboratory for Physical Sciences at the Microscale and Synergetic Innovation Center of Quantum Information and Quantum Physics, University of Science and Technology of China, Hefei, Anhui 230026, China*

²*Synergetic Innovation Center of Quantum Information and Quantum Physics, University of Science and Technology of China, Hefei, Anhui 230026, China*

³*Department of Physics, University of California, San Diego, La Jolla, California 92093, USA*

(Dated: Submitted on July 30, 2020)

Measuring local temperatures of open systems out of equilibrium is emerging as a novel approach to study the local thermodynamic properties of nanosystems. An operational protocol has been proposed to determine the local temperature by coupling a probe to the system and then minimizing the perturbation to a certain local observable of the probed system. In this paper, we first show that such a local temperature is unique for a single quantum impurity and the given local observable. We then extend this protocol to open systems consisting of multiple quantum impurities by proposing a local minimal perturbation condition (LMPC). The influence of quantum resonances on the local temperature is elucidated by both analytic and numerical results. In particular, we demonstrate that quantum resonances may give rise to strong oscillations of the local temperature along a multi-impurity chain under a thermal bias.

I. INTRODUCTION

Local temperatures of systems out of equilibrium¹ are of fundamental importance in many sub-fields of modern science, including physics,^{2–5} chemistry^{6–8} and biology.^{9–11} With the development of high-resolution thermometric techniques,^{4,12,13} the measurement of local temperature distributions in nonequilibrium nanoscopic systems has been realized, such as in graphene-metal contacts,¹⁴ aluminum nanowires,¹³ and two-dimensional metallic films.¹⁵

A nonequilibrium system under an external driving source, such as a bias voltage or a thermal gradient, often possesses a local temperature somewhat higher than the background temperature.¹⁶ Such a local heating effect usually originates from the electronic and phononic excitations occurring in the system, and has significant influence on some physical properties¹⁷ and processes.^{18–23}

From theoretical perspective, extending the concept of temperature from equilibrium systems to local subregions of nonequilibrium systems can be based on the following considerations:^{1,24–41} (i) Local temperature can be defined by presuming the validity of a local equilibrium approximation. In the context of the zeroth law of thermodynamics, such an approximation indicates that there is no net flow of particle or energy between the local system and its surrounding environment. (ii) Local temperature can be associated with an energy scale that characterizes the magnitude of local excitations. Thus, the deviation of local temperature from the background temperature quantifies how far the system is away from a global equilibrium state. (iii) Local temperature can be determined by probing the variation of intrinsic thermodynamic or dynamic properties of the local system.

Ideally, the definition of local temperature should be universal (so that it can be applied to as many nonequilibrium situations as possible), unique (so that it yields

one and only one value of temperature), operationally feasible (so that it can be measured experimentally), and has the correct asymptotic limit (so that it retrieves the thermodynamic temperature as the system approaches towards an equilibrium state).¹

For instance, Engquist and Anderson defined the local temperature based on a local equilibrium condition⁴² referred to as zero-current condition (ZCC) in this paper. In this definition, an ideal potentiometer/thermometer (the probe) is weakly coupled to the nonequilibrium system of interest. By varying the temperature (T_p) and chemical potential (μ_p) of the probe until both the electric (I_p) and heat currents (J_p) flowing through the probe vanish, the local temperature (T^*) and local chemical potential (μ^*) of the system are determined as $T^* = T_p$ and $\mu^* = \mu_p$, respectively. This protocol has been used widely to investigate the local temperature^{43–47} and local electrochemical potential distribution^{48–50} of nanosystems out of equilibrium.

The ZCC-based definition has been employed to study the distribution of local temperature along a nanowire connected to macroscopic electron reservoirs.^{51–53} It is interesting to find that the local temperature profile exhibits a periodic oscillation along the nanowire.⁵² The oscillatory behavior was predicted to occur from the emergence of quantum coherence as the size of the system reduces to be comparable to or even smaller than the mean free path of electrons.⁵⁴ Therefore, the energy transport process in a nanojunction is significantly different from that in a bulk system, and consequently the classical Fourier's law is strongly violated.^{1,55–58} Such quantum oscillations have also been observed in some other systems, such as the conjugated organic molecules⁵⁹ and graphene nanostructures.⁶⁰

The ZCC-based definition has the advantage of yielding a unique value of local temperature ($T^{*,ZCC}$) for any nonequilibrium system.⁶¹ However, its experimental re-

alization is rather challenging because of the difficulty in measuring the heat current through a nano-sized sample without knowing its priori local temperature.¹ Moreover, the effectiveness of the ZCC-based definition is questionable if the energy level of the system is in *quantum resonance* with the states of the environment. This is because if the electron or energy transport is dominated by quantum resonant states, the excitations pertinent to the nonequilibrium processes are *highly nonlocal*, and hence the local equilibrium approximation which forms the basis of $T^{*,ZCC}$ may no longer be valid. Indeed, it has been shown that the $T^{*,ZCC}$ of a single-level quantum dot vary very little as the dot level shifts from the off-resonance to resonance region.⁶² Therefore, $T^{*,ZCC}$ fail to reflect the quantum resonance feature of a nonequilibrium system.

Alternatively, an operational protocol to determine the local temperature has been proposed, which is based on a minimal-perturbation condition (MPC).^{54,62,63} In this protocol, a probe is weakly coupled to the system, and concomitantly a certain system observable (O) is monitored. The local temperature and local chemical potential are determined by varying the T_p and μ_p until the perturbation on the system observable O caused by the probe gets minimized. The MPC-based protocol does not require the direct measurement of heat current, and hence its experimental realization is straightforward.

It has been demonstrated that, for a single-level quantum dot, the $T^{*,MPC}$ determined by monitoring different system observables coincide with each other and agree closely with the $T^{*,ZCC}$ in the absence of quantum resonance.⁶² This is because a quantitative correspondence can be established based on the $T^{*,MPC}$ between the nonequilibrium system of interest and a reference system in thermal equilibrium, provided that the pertinent system observable and excitations are fully local. However, in contrast to the $T^{*,ZCC}$, the $T^{*,MPC}$ determined by certain observables exhibit sharp variations in the near resonance region.^{62,63} This indicates that the $T^{*,MPC}$ have the potential of resolving the quantum resonance features of a nonequilibrium system.

Despite the effectiveness and feasibility of the MPC-based definition, there are still issues that remain unclear. Some of them are as follows: (i) Does the MPC predict a unique value of T^* ? (ii) When and why do $T^{*,MPC}$ coincide with $T^{*,ZCC}$ in the absence of quantum resonances? (iii) So far the application of the MPC has been restricted to systems containing a single impurity. How do we extend the definition of $T^{*,MPC}$ to multi-impurity systems? (iv) Do quantum resonances lead to any discernible feature in the distribution of local temperatures along a quantum wire?

This work aims at elucidating the above issues through theoretical analysis and numerical calculations. In particular, to address the last two questions, we propose a local minimal-perturbation condition (LMPC) by imposing explicitly the nonequilibrium-equilibrium correspondence relation. As a direct extension of the original MPC, the LMPC enables the determination of the local temper-

ature and local chemical potential of each impurity in a multi-impurity system out of equilibrium.

The remainder of this paper is organized as follows. In Sec. II, we revisit the MPC protocol and discuss how to reach a unique prediction of the local temperature of a single quantum impurity. In Sec. III, we propose the LMPC-based definition of local temperature. As a numerical example we calculate the distribution of local temperatures along a quantum wire consisting of four impurities. Concluding remarks are given in Sec. IV.

II. EFFECT OF QUANTUM RESONANCES ON LOCAL TEMPERATURES OF SINGLE IMPURITY SYSTEMS

A. Quantum impurity systems

In the following, the Anderson impurity models (AIMs)⁶⁴ are adopted to describe the open systems. The total Hamiltonian of the system-plus-environment is

$$\hat{H} = \hat{H}_{\text{imp}} + \hat{H}_{\text{lead}} + \hat{H}_{\text{coup}}, \quad (1)$$

where the three terms on the right-hand side (RHS) represent the Hamiltonian of the impurities, the Hamiltonian of the leads which serve as the electron reservoirs and heat baths, and the Hamiltonian of the impurity-lead couplings, respectively.

We consider first a single impurity described by $\hat{H}_{\text{imp}} = \epsilon_d \hat{n} + U \hat{n}_\uparrow \hat{n}_\downarrow$. Here, $\hat{n} = \sum_s \hat{n}_s = \sum_s \hat{a}_s^\dagger \hat{a}_s$, with \hat{a}_s^\dagger (\hat{a}_s) creating (annihilating) an electron of spin s on the impurity level ϵ_d , and U is the Coulomb interaction energy between the spin-up and spin-down electrons. $\hat{H}_{\text{lead}} = \sum_{\alpha ks} \epsilon_{\alpha k} \hat{d}_{\alpha ks}^\dagger \hat{d}_{\alpha ks}$ and $\hat{H}_{\text{coup}} = \sum_{\alpha ks} t_{\alpha k} \hat{a}_s^\dagger \hat{d}_{\alpha ks} + \text{H.c.}$ describe the noninteracting leads and the impurity-lead coupling, respectively. Here, $\hat{d}_{\alpha ks}^\dagger$ ($\hat{d}_{\alpha ks}$) creates (annihilates) a spin- s electron on the k th orbital of the α th lead, and $t_{\alpha k}$ is the coupling strength between the impurity level and the k th lead orbital.

To investigate the properties of the impurity, the hierarchical equations of motion (HEOM) approach⁶⁵⁻⁷⁰ is employed, which takes the reduced density matrix of the system ρ and a hierarchical set of auxiliary density operators as the basic variables. The HEOM theory is, in principle, formally exact, and its numerical outcomes are guaranteed to be quantitatively accurate if the results converge with respect to the truncation tier of the hierarchy.^{71,72} The HEOM approach has been widely used to study a variety of static and dynamic properties of strongly correlated quantum impurity systems in and out of equilibrium.^{62,63,73-79}

In the framework of the HEOM, the influence of the noninteracting leads on the impurity is fully captured by the hybridization functions, $\Gamma_\alpha(\omega) \equiv \pi \sum_k |t_{\alpha k}|^2 \delta(\omega - \epsilon_{\alpha k})$. For numerical convenience, a Lorentzian form of $\Gamma_\alpha(\omega) = \frac{\Delta_\alpha W_\alpha^2}{(\omega - \Omega_\alpha)^2 + W_\alpha^2}$ is adopted, where Δ_α is the effec-

tive coupling strength between the impurity and the α th lead, and Ω_α and W_α are the band center and width of the α th lead, respectively. We further set the band center at the chemical potential of the lead, i.e., $\Omega_\alpha = \mu_\alpha$. The chemical potential of the equilibrium composite system is set to the zero energy, i.e., $\mu^{\text{eq}} = 0$.

In the following, Δ_p (the subscript p denotes the probe) is taken to be at least two orders of magnitude smaller than all the other Δ_α , and further reducing its value does not influence the resulting T^* and μ^* .⁶³ Hereafter, we adopt the atomic units $e = \hbar = k_B \equiv 1$; and $\Delta = \sum_{\alpha \neq p} \Delta_\alpha$ is taken as the unit of energy.

B. Minimal-perturbation condition

Consider the scenario that a single impurity is coupled to the left (L) and right (R) leads, whose background temperatures (chemical potentials) are T_L and T_R (μ_L and μ_R), respectively. By coupling an external probe to the impurity, the local observable $O = \langle \hat{O} \rangle = \text{tr}(\hat{O}\rho)$ is subject to a perturbation of

$$\delta O_p = O_p(T_p, \mu_p) - O_{\text{ref}}. \quad (2)$$

Here, $O_p(T_p, \mu_p)$ is the value of O measured by setting the temperature and chemical potential of the coupled probe to T_p and μ_p , respectively. O_{ref} is the minimally perturbed value of O which serves as reference for O_p . For a single-impurity system, O_{ref} is determined by

$$O_{\text{ref}} = \zeta_L O_p(T_L, \mu_L) + \zeta_R O_p(T_R, \mu_R), \quad (3)$$

where the coefficients ζ_α ($\alpha = L$ and R) are acquired as⁶³

$$\zeta_\alpha = 1 - \left| \frac{I_p(T_\alpha, \mu_\alpha)}{I_p(T_L, \mu_L) - I_p(T_R, \mu_R)} \right|. \quad (4)$$

Here, $I_p(T_p, \mu_p)$ is the electric current flowing into the probe with its temperature and chemical potential set to T_p and μ_p , respectively. For AIMs, $\zeta_\alpha = \frac{\Delta_\alpha}{\Delta_L + \Delta_R}$.

The local temperature T^* and local chemical potential μ^* of the impurity are determined by

$$\begin{cases} I_p(T^*, \mu^*) = 0 \\ (T^*, \mu^*) = \arg \min_{(T_p, \mu_p)} |\delta O_p(T_p, \mu_p)|. \end{cases} \quad (5)$$

In particular, if $\delta O_p = 0$ is achievable by tuning T_p and μ_p , the MPC actually becomes the zero perturbation condition (ZPC). The definition of Eq. (5) does not involve the troublesome heat current, and all the involving quantities (e.g. I_p and O_p) can be measured directly in experiments. Therefore, Eq. (5) provides an operational protocol for the determination of T^* and μ^* . In practice, such a protocol for the system under a bias voltage may be further simplified with a preset μ^* as follows,

$$\begin{cases} \mu^* \approx \zeta_L \mu_L + \zeta_R \mu_R \\ T^* = \arg \min_{T_p} |\delta O_p(T_p, \mu^*)|. \end{cases} \quad (6)$$

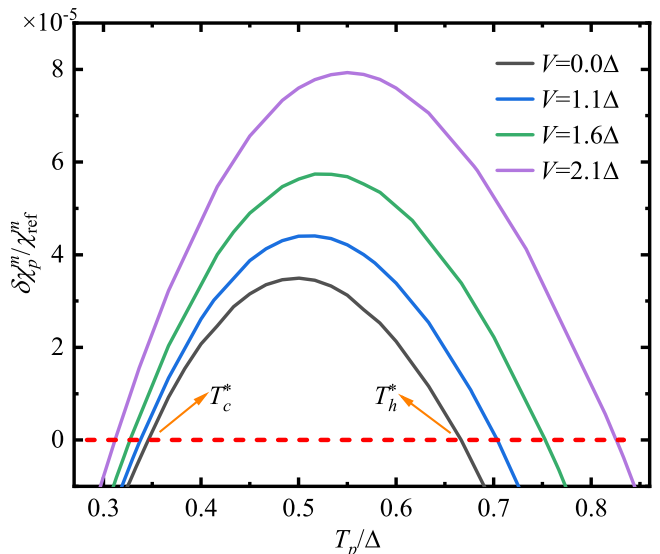


FIG. 1. $\delta\chi_p^m/\chi_{\text{ref}}^m$ as a function of T_p for a single-impurity system under an antisymmetric bias voltage of $\mu_R = -\mu_L = V/2$. T_c^* and T_h^* are two temperatures which satisfy the ZPC of $\delta\chi_p^m = 0$, as indicated by the horizontal line. The energetic parameters of the system are (in units of Δ): $T_L = T_R = 0.67$, $\epsilon_d = -3.33$, $\Delta_L = \Delta_R = 0.5$, $U = 2.5$, and $W_L = W_R = 6.67$.

For a convenient and accurate measurement of T^* , the local observable O should vary sensitively with T_p . In our previous works,^{62,63} the local magnetic and charge susceptibilities of the impurity, $\chi^m = \frac{\partial \langle \hat{n}_z \rangle}{\partial H_z} |_{H_z \rightarrow 0}$ and $\chi^c = -\frac{\partial \langle \hat{n} \rangle}{\partial \epsilon_d}$, respectively, have been chosen as the local observables. Here, $\hat{n}_z = \frac{1}{2}g\mu_B(\hat{n}_\uparrow - \hat{n}_\downarrow)$ is the impurity magnetization operator, with H_z being the local magnetic field, g the electron gyromagnetic ratio, and μ_B the Bohr magneton. It has been shown that while $T^{*,\text{MPC}}(\chi^m)$ and $T^{*,\text{MPC}}(\chi^c)$ agree closely with each other in most cases, they do exhibit small discrepancy in the near-resonance (NR) region.⁶²

In the following, we explore the uniqueness/non-uniqueness of the $T^{*,\text{MPC}}$. First, we show that the MPC of Eq. (5) or Eq. (6) may give rise to multiple values of T^* with a certain O . Figure 1 depicts the relative perturbation of local magnetic susceptibility, $\delta\chi_p^m/\chi_{\text{ref}}^m$, as a function of T_p for a single-impurity system under an antisymmetric bias voltage. From the first line of Eq. (6) we have $\mu^* = 0$ since $\Delta_L = \Delta_R$. Meanwhile, it is intriguing to find that there are two temperatures that could satisfy the ZPC of $\delta\chi_p^m = 0$, which are designated as T_c^* and T_h^* ($T_c^* < T_h^*$). Thus, the local temperature $T^{*,\text{MPC}}$ appears to be non-unique. However, it is important to note that, the whole system should approach towards an equilibrium state as the bias voltage is reduced gradually. In particular, in the limit of $V \rightarrow 0$, $T^{*,\text{MPC}}$ should recover the thermodynamic temperature of the equilibrium system, i.e., $T^{*,\text{MPC}} = T_L = T_R$. In Fig. 1 it is evident that only T_h^* achieves the correct asymptotic limit at the

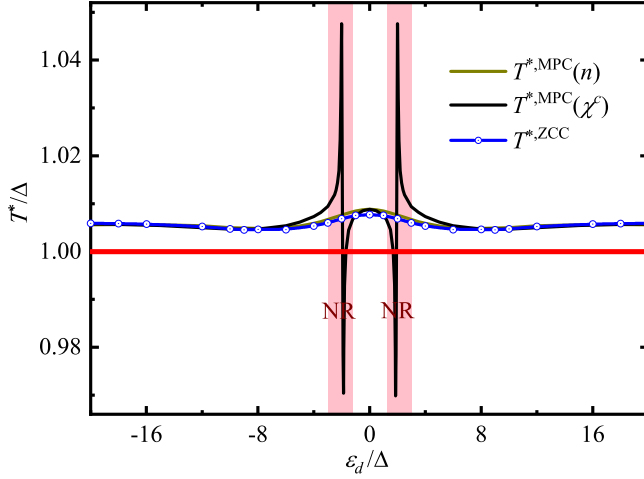


FIG. 2. $T^{*,\text{MPC}}(n)$, $T^{*,\text{MPC}}(\chi^c)$ and $T^{*,\text{ZCC}}$ versus ϵ_d for a noninteracting single-impurity system under an antisymmetric bias voltage of $\mu_R = -\mu_L = V/2 = 0.2\Delta$. The energetic parameters of the system are (in units of Δ): $T_L = T_R = 1$, $U = 0$, $\Delta_L = \Delta_R = 0.5$, and $W_L = W_R = 50$. The shaded areas represent the near-resonance (NR) regions.

zero bias. Therefore, although the MPC of Eq.(6) has multiple solutions, the local temperature $T^{*,\text{MPC}}$ turns out to be unique by considering the asymptotic limit of the global equilibrium state.

C. Effect of quantum resonances on local temperature

We then explore the uniqueness/non-uniqueness of $T^{*,\text{MPC}}$ associated with different local observables in the off-resonance, near-resonance, and resonance regions. To this end, we consider a noninteracting single-impurity system under an antisymmetric bias voltage. Figure 2 depicts the variation of $T^{*,\text{MPC}}$ determined by Eq. (6) with the change of ϵ_d . The displayed $T^{*,\text{MPC}}$ are associated with the electron occupation number on the impurity $n = \langle \hat{n} \rangle$ or with the local charge susceptibility χ^c . In both cases, we have $\mu^{*,\text{MPC}} = 0$ since $\Delta_L = \Delta_R$. For comparison, the $T^{*,\text{ZCC}}$ versus ϵ_d are also shown in Fig. 2.

From Fig. 2, it is clear that $T^{*,\text{ZCC}}$ and $T^{*,\text{MPC}}(n)$ vary smoothly and coincide closely with each other over the whole range of ϵ_d . In contrast, while the $T^{*,\text{MPC}}(\chi^c)$ agree well with the other two local temperatures in the off-resonance regions ($|\epsilon_d|$ is far away from the chemical potentials of leads), they exhibit strong oscillations in the NR regions. Such oscillations reflect the emergence of nonlocal excitations as a quantum resonant state begins to establish in the system.⁶² Consequently, $T^{*,\text{MPC}}$ may serve as an indicator for the appearance of quantum resonances, if the magnitude of the associated local observable O varies sensitively with nonlocal excitations.

To understand the quantitative agreement between

$T^{*,\text{MPC}}(n)$ and $T^{*,\text{ZCC}}$ in Fig. 2, we carry out some theoretical analysis by using the nonequilibrium Green's function (NEGF) method. In the wide-band limit ($W \rightarrow \infty$), the spin- s component of the steady-state electric current flowing into the probe is

$$\begin{aligned} I_{ps} &= -\frac{i}{\pi} \int d\omega \Gamma_p(\omega) \{G_s^<(\omega) + 2i f_{T_p, \mu_p}(\omega) \text{Im}[G_s^r(\omega)]\} \\ &= \frac{2\Delta_p \Delta}{\Delta + \Delta_p} \int d\omega A_s(\omega) [\zeta_L f_{T_L, \mu_L}(\omega) \\ &\quad + \zeta_R f_{T_R, \mu_R}(\omega) - f_{T_p, \mu_p}(\omega)], \end{aligned} \quad (7)$$

and the electron occupation number on the impurity is

$$\begin{aligned} n &= \sum_s n_s = \sum_s \frac{1}{2\pi i} \int d\omega G_s^<(\omega) \\ &= \sum_\alpha \frac{\Delta_\alpha}{\Delta + \Delta_p} \int d\omega A(\omega) f_{T_\alpha, \mu_\alpha}(\omega). \end{aligned} \quad (8)$$

Here, $G_s^r(\omega)$ and $G_s^<(\omega)$ are the retarded and lesser single-electron Green's functions of the impurity, respectively; $A(\omega) = \sum_s A_s(\omega) = -\frac{1}{\pi} \sum_s \text{Im}[G_s^r(\omega)]$ is the spectral function of the impurity; and $f_{T_\alpha, \mu_\alpha}(\omega)$ is the Fermi distribution function.

The ZPC for the local observable $n = \langle \hat{n} \rangle$ is expressed as

$$\begin{aligned} \delta n_p &= n_p(T_p, \mu_p) - n_{\text{ref}} \\ &= \frac{\Delta_p}{\Delta + \Delta_p} \int d\omega A(\omega) \{f_{T_p, \mu_p}(\omega) \\ &\quad - [\zeta_L f_{T_L, \mu_L}(\omega) + \zeta_R f_{T_R, \mu_R}(\omega)]\} \\ &= 0. \end{aligned} \quad (9)$$

By comparing Eqs. (7) and (9), it is immediately recognized that the ZPC for the observable n is exactly equivalent to the ZCC of $I_p = \sum_s I_{ps} = 0$.

On the other hand, unlike the presumed $\mu^{*,\text{MPC}}(n) = 0$, the ZCC also requires zero heat current, $J_p = 0$, which often gives rise to a nonzero $\mu^{*,\text{ZCC}}$. Such a minor difference in μ^* in turn leads to the slightly different T^* . Consequently, as shown in Fig. 2, the resulting $T^{*,\text{ZCC}}$ are very close but not exactly equal to $T^{*,\text{MPC}}(n)$.

We now elaborate on the quantitative agreement between $T^{*,\text{MPC}}(n)$ and $T^{*,\text{MPC}}(\chi^c)$ apart from the NR regions. In the NEGF formalism the local charge susceptibility is expressed as

$$\chi^c = -\sum_\alpha \frac{\Delta_\alpha}{\Delta + \Delta_p} \int d\omega \frac{\partial A(\omega)}{\partial \epsilon_d} f_{T_\alpha, \mu_\alpha}(\omega), \quad (10)$$

and its perturbation by the coupled probe is

$$\begin{aligned} \delta \chi_p^c &= \chi_p^c(T_p, \mu_p) - \chi_{\text{ref}}^c \\ &= -\frac{\Delta_p}{\Delta + \Delta_p} \int d\omega \frac{\partial A(\omega)}{\partial \epsilon_d} \{f_{T_p, \mu_p}(\omega) \\ &\quad - [\zeta_L f_{T_L, \mu_L}(\omega) + \zeta_R f_{T_R, \mu_R}(\omega)]\}. \end{aligned} \quad (11)$$

From Eqs. (9) and (11) it is clear that the probe-induced perturbation to any local observable O can be cast into a general form of

$$\delta O_p = \int d\omega g_1(\omega, T_p) g_2^O(\omega, \epsilon_d), \quad (12)$$

with

$$\begin{aligned} g_1(\omega, T_p) &= f_{T_p, \mu_p}(\omega) - [\zeta_L f_{T_L, \mu_L}(\omega) + \zeta_R f_{T_R, \mu_R}(\omega)] \\ &= \frac{1}{1 + e^{\omega/T_p}} - \frac{1}{2[1 + e^{(\omega+V/2)/T_L}]} \\ &\quad - \frac{1}{2[1 + e^{(\omega-V/2)/T_R}]} \end{aligned} \quad (13)$$

being a window function centered at $\omega = 0$. Here, the second equality holds because we have $\zeta_L = \zeta_R = \frac{1}{2}$ and $\mu_p = \mu^* = 0$ in the case of $\Delta_L = \Delta_R$ and $\mu_R = -\mu_L = \frac{V}{2}$.

In Eq. (12), the form of the function $g_2^O(\omega, \epsilon_d)$ depends on the definition of the local observable O . Specifically, since the spectral function of a noninteracting impurity in the presence of a weakly coupled probe is

$$A(\omega) = \frac{2}{\pi} \frac{\Delta + \Delta_p}{(\omega - \epsilon_d)^2 + (\Delta + \Delta_p)^2}, \quad (14)$$

we have

$$\begin{aligned} g_2^n(\omega, \epsilon_d) &= \frac{2\Delta_p}{\pi} \frac{1}{(\omega - \epsilon_d)^2 + (\Delta + \Delta_p)^2}, \quad (15) \\ g_2^\chi(\omega, \epsilon_d) &= -\frac{\partial g_2^n}{\partial \epsilon_d} = -\frac{4\Delta_p}{\pi} \frac{\omega - \epsilon_d}{[(\omega - \epsilon_d)^2 + (\Delta + \Delta_p)^2]^2}. \end{aligned} \quad (16)$$

By combining Eq. (6) and Eq. (12), the $T^{*,\text{MPC}}(O)$ is determined by tuning T_p until the following ZPC is met:

$$\delta O_p = \int d\omega g_1(\omega, T_p) g_2^O(\omega, \epsilon_d) = 0, \quad (17)$$

With $T_L = T_R$, $g_1(\omega, T_p)$ is an odd function of ω , and its nontrivial values appear only in a nonequilibrium activation window centered at $\omega = 0$.

Off-resonance– The impurity system is in the off-resonance region if the impurity energy level ϵ_d is far away from the nonequilibrium activation window defined by $g_1(\omega, T_p)$. In such a case, it is the tail of g_2^O that overlaps the main body of g_1 . Since $g_2^O(\omega, \epsilon_d)$ varies rather smoothly with ω in the nonequilibrium activation window, we may use the Taylor expansion and rewrite the ZPC of Eq. (17) as

$$\begin{aligned} \delta O_p &= \int d\omega g_1(\omega, T_p) \left[g_2^O(0, \epsilon_d) + \partial_\omega g_2^O(0, \epsilon_d) \omega \right. \\ &\quad \left. + \frac{1}{2} \partial_\omega^2 g_2^O(\xi, \epsilon_d) \omega^2 \right] \\ &= \partial_\omega g_2^O(0, \epsilon_d) \int d\omega g_1(\omega, T_p) \omega \\ &= 0. \end{aligned} \quad (18)$$

Here, $\partial_\omega \equiv \frac{\partial}{\partial \omega}$ and $\partial_\omega^2 \equiv \frac{\partial^2}{\partial \omega^2}$, and $\partial_\omega^2 g_2^O(\xi, \epsilon_d)$ with $\xi \in (0, \omega)$ is the Lagrange remainder. The first equality uses the fact that $g_1(\omega, T_p)$ is an odd function of ω . It is thus evident that, for the single-impurity system under study, the ZPC holds *universally* for any local observable in the off-resonance region, i.e., $T^{*,\text{MPC}}(n) = T^{*,\text{MPC}}(\chi^c) = T^{*,\text{MPC}}(O)$ for any O .

In-resonance– In contrast, the impurity system is in the resonance region if ϵ_d is close to the lead chemical potential and thus lies within the nonequilibrium activation window. In this case, the value of $T^{*,\text{MPC}}(O)$ may vary with the specific choice of O , since different local observables may respond differently to nonlocal excitations. Instead, we still see $T^{*,\text{MPC}}(n) \approx T^{*,\text{MPC}}(\chi^c)$ in Fig. 2. This is because of the following relation resulting from the Taylor expansion and the first equality of Eq. (16),

$$\begin{aligned} g_2^n(\omega, \epsilon_d) &= g_2^n(\omega, 0) - \epsilon_d g_2^\chi(\omega, \xi_1) \\ &= g_2^n(\omega, 0) - \epsilon_d g_2^\chi(\omega, \epsilon_d) \\ &\quad - \epsilon_d (\xi_1 - \epsilon_d) \partial_{\epsilon_d} g_2^\chi(\omega, \xi_2). \end{aligned} \quad (19)$$

Here, $\xi_1 \in (0, \epsilon_d)$ and $\xi_2 \in (\xi_1, \epsilon_d)$. $g_2^n(\omega, 0)$ is an even function of ω and its overlap integral with $g_1(\omega, T_p)$ is zero. The last term on the RHS of Eq. (19) is negligibly small since $\epsilon_d (\xi_1 - \epsilon_d) \sim \mathcal{O}(\epsilon_d^2)$ and $\partial_{\epsilon_d} g_2^\chi(\omega, \xi_2)$ is nearly an even function of ω . Therefore, by combining Eq. (17) and Eq. (19), we find that the ZPC for n is approximately equivalent to the ZPC for χ^c , and hence $T^{*,\text{MPC}}(n) \approx T^{*,\text{MPC}}(\chi^c)$.

Near-resonance– In the NR region, the product of $g_1(\omega, T_p)$ and $g_2^O(\omega, \epsilon_d)$ depends sensitively on the nature of O , and so is the value of $T^{*,\text{MPC}}$; see Fig. 2.

From the above theoretical analysis we can conclude that the choice of local observable has little influence on $T^{*,\text{MPC}}$ in the off-resonance regions. In contrast, in the resonance or NR region, the value of $T^{*,\text{MPC}}$ depends on how significantly the local observable is affected by the emerging nonlocal excitations and how sensitively it varies with T_p .

When quantum resonances come into play, the notion of “local equilibrium” is no longer appropriate, and the nonlocal excitations cannot be properly characterized by $T^{*,\text{ZCC}}$. In contrast, $T^{*,\text{MPC}}$ measured by monitoring a suitable local observable (such as the $T^{*,\text{MPC}}(\chi^c)$ depicted in Fig. 2) are *still* capable of identifying and quantifying the magnitude of the nonlocal excitations. Even in the NR or resonance region, the $T^{*,\text{MPC}}(O)$ still carry an unambiguous thermodynamic meaning manifested through a correspondence relation,⁶² i.e., the local observable O of the measured nonequilibrium system is identical to that of a reference system in an equilibrium state with the temperature $T^{*,\text{MPC}}(O)$.

III. EFFECT OF QUANTUM RESONANCES ON LOCAL TEMPERATURES OF MULTI-IMPURITY SYSTEMS

A. Local minimal-perturbation condition

We now extend the MPC to the systems consisting of more than one impurity. Consider a serially coupled N -impurity system described by an AIM with

$$\hat{H}_{\text{imp}} = \sum_{i=1}^N \epsilon_i \hat{n}_i + \sum_{i=1}^N U \hat{n}_{i\uparrow} \hat{n}_{i\downarrow} + \sum_{i=1}^{N-1} [t (\hat{a}_{i\uparrow}^\dagger \hat{a}_{i+1\uparrow} + \hat{a}_{i\downarrow}^\dagger \hat{a}_{i+1\downarrow}) + \text{H.c.}], \quad (20)$$

where ϵ_i is the on-site energy of the i th impurity, and t is the coupling strength between two adjacent impurities. As illustrated in Fig. 3(a), the N -impurity system forms a linear chain, in which the left (right) lead is coupled only to the 1st (N th) impurity with the coupling strength being Δ_L (Δ_R).

In principle the MPC of Eq. (5) can be formally extended to determine the local temperature and local chemical potential of each individual impurity as follows,

$$\begin{cases} I_{p,i}(T_i^*, \mu_i^*) = 0, \\ (T_i^*, \mu_i^*) = \arg \min_{(T_p, \mu_p)} |\delta O_{p,i}(T_p, \mu_p)|. \end{cases} \quad (21)$$

Here, the probe is weakly coupled to the i th impurity. As a natural extension of the MPC, Eq. (21) is referred to as the local MPC (LMPC). However, in practice the extension from MPC to LMPC is not always straightforward. This is because it is often difficult to acquire the minimally perturbed value of a particular local observable $O_{\text{ref},i}$. To circumvent this problem, we can choose a local observable whose reference value is known by the intrinsic symmetry of the system.

For instance, if the investigated multi-impurity system is spin-unpolarized, i.e., all the energetic parameters in Eq. (20) are spin-independent, by coupling a probe to an impurity, the electric current through the probe should also be spin-unpolarized. In other words, if the local observable O is chosen to be the magnetic susceptibility of the electric current through the coupled probe, $\chi_{p,i}^I \equiv \frac{\partial I_{pz,i}}{\partial H_z} |_{H_z \rightarrow 0}$ with $I_{pz,i} = \frac{1}{2}(I_{p,i\uparrow} - I_{p,i\downarrow})$, its minimally perturbed value is just $\chi_{\text{ref},i}^I = 0$, if the i th impurity is spin-unpolarized in the presence of the probe. Note that for the measurement of (T_i^*, μ_i^*) the magnetic field H_z is applied exclusively on the i th impurity.

For a single-impurity system, the thermodynamic meaning of $T^{*,\text{MPC}}$ has been elucidated via a correspondence condition between the nonequilibrium system under study and a reference system in thermal equilibrium, i.e., $O_{\text{neq}} = O_{\text{eq}}$, provided that the $T^{*,\text{MPC}}(O)$ and $\mu^{*,\text{MPC}}(O)$ of the nonequilibrium system coincide with the equilibrium temperature and chemical potential of the reference system.⁶²

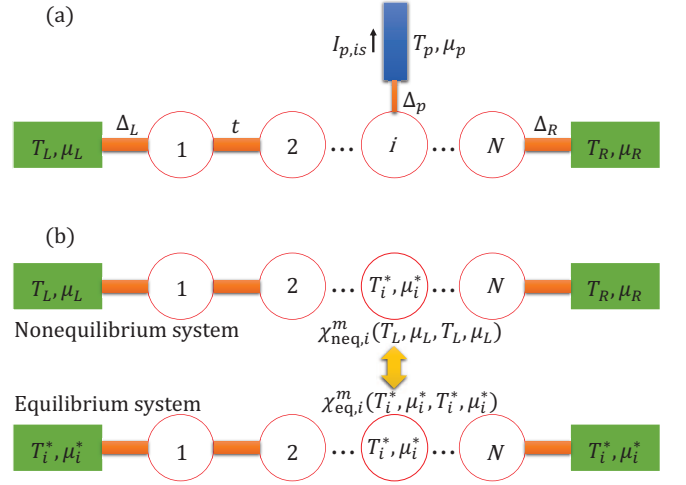


FIG. 3. (a) Schematic illustration of a serially coupled N -impurity system. The first (N th) impurity is coupled to the left (right) lead. The probe is weakly coupled to the i th impurity under study, and the spin-specific electric current flowing into the probe $I_{p,is}$ is monitored. (b) Schematic illustration of the correspondence relation which states that the local magnetic susceptibility of the i th impurity in a nonequilibrium system is equal to that in an equilibrium system, provided that they have the same local temperature and local chemical potential.

In the following, we demonstrate that a correspondence relation can also be established for a multi-impurity system with the $\chi_{p,i}^I$ chosen as the local observable.

To facilitate the theoretical analysis, we consider a serially coupled noninteracting double-impurity system. By applying a local magnetic field H_z to the i th impurity, the impurity level is subject to a Zeeman splitting which is assumed to be linearly proportional to H_z . Consequently, for the spin-unpolarized system under study, we have $\chi_{p,i}^I = C \frac{\partial I_{p,i\uparrow}}{\partial \epsilon_i}$ with C being a constant. Without loss of generality, the probe is coupled to the first impurity. In the wide-band limit, the probe-induced perturbation to $\chi_{p,1}^I$ is expressed as

$$\begin{aligned} \delta \chi_{p,1}^I &= -C \frac{i}{\pi} \int d\omega \Gamma_p(\omega) \partial_{\epsilon_1} \left\{ G_{\uparrow,11}^<(\omega) \right. \\ &\quad \left. + 2i f_{T_p, \mu_p}(\omega) \text{Im}[G_{\uparrow,11}^r(\omega)] \right\} \\ &= C \frac{2\Delta_p}{\pi} \int d\omega \left\{ \Delta_L [(\omega - \epsilon_2)^2 + \Delta_R^2] \right. \\ &\quad \times [f_{T_L, \mu_L}(\omega) - f_{T_p, \mu_p}(\omega)] + t^2 \Delta_R \\ &\quad \left. \times [f_{T_R, \mu_R}(\omega) - f_{T_p, \mu_p}(\omega)] \right\} \partial_{\epsilon_1} |B_{p1}(\omega)|^2, \quad (22) \end{aligned}$$

where

$$B_{p1}(\omega) = \frac{1}{[\omega - \epsilon_1 + i(\Delta_L + \Delta_p)](\omega - \epsilon_2 + i\Delta_R) - t^2}. \quad (23)$$

Similarly, for a spin-unpolarized system, the local magnetic susceptibility of the i th impurity can be rewritten

as $\chi_i^m = \mathcal{C}' \frac{\partial n_{i\uparrow}}{\partial \epsilon_i}$, with \mathcal{C}' being a constant different from \mathcal{C} . In the nonequilibrium steady state characterized by the temperatures and chemical potentials of the left and right leads, (T_L, μ_L, T_R, μ_R) , the value of χ_1^m in the absence of the probe is

$$\begin{aligned} \chi_{\text{neq},1}^m &= \mathcal{C}' \frac{1}{2\pi i} \int d\omega \partial_{\epsilon_1} [G_{\uparrow,11}^<(\omega)] \\ &= \mathcal{C}' \frac{1}{\pi} \int d\omega \left\{ \Delta_L [(\omega - \epsilon_2)^2 + \Delta_R^2] f_{T_L, \mu_L}(\omega) \right. \\ &\quad \left. + t^2 \Delta_R f_{T_R, \mu_R}(\omega) \right\} \partial_{\epsilon_1} |B(\omega)|^2, \end{aligned} \quad (24)$$

where $B(\omega) = B_{p1}(\omega)|_{\Delta_p=0}$. For the reference system in a thermal equilibrium state characterized by the background temperature T_1^* and chemical potential μ_1^* , the corresponding χ_1^m is expressed in a form similar to Eq. (24), but with (T_L, μ_L, T_R, μ_R) replaced by $(T_1^*, \mu_1^*, T_1^*, \mu_1^*)$. Therefore, the difference between $\chi_{\text{neq},1}^m$ and $\chi_{\text{eq},1}^m$ is

$$\begin{aligned} &\chi_{\text{neq},1}^m(T_L, \mu_L, T_R, \mu_R) - \chi_{\text{eq},1}^m(T_1^*, \mu_1^*, T_1^*, \mu_1^*) \\ &= \frac{\mathcal{C}'}{\pi} \int d\omega \left\{ \Delta_L [(\omega - \epsilon_2)^2 + \Delta_R^2] [f_{T_L, \mu_L}(\omega) - f_{T_1^*, \mu_1^*}(\omega)] \right. \\ &\quad \left. + t^2 \Delta_R [f_{T_R, \mu_R}(\omega) - f_{T_1^*, \mu_1^*}(\omega)] \right\} \partial_{\epsilon_1} |B(\omega)|^2. \end{aligned} \quad (25)$$

By comparing Eq. (22) and Eq. (25), it is easy to recognize that the relation

$$\chi_{\text{neq},1}^m(T_L, \mu_L, T_R, \mu_R) = \chi_{\text{eq},1}^m(T_1^*, \mu_1^*, T_1^*, \mu_1^*) \quad (26)$$

holds provided that

$$\left. \frac{\delta \chi_{p,1}^I(T_1^*, \mu_1^*)}{\Delta_p} \right|_{\Delta_p \rightarrow 0} = 0. \quad (27)$$

A similar relation can be established for the second impurity of the double-impurity system, or any impurity of a generic multi-impurity system; see Fig. 3(b).

Equation (27) is the local ZPC for the local observable $\chi_{p,1}^I$, and the thermodynamic meaning of the resulting (T_1^*, μ_1^*) is unambiguously given by Eq. (26). When the local ZPC of Eq. (27) cannot be reached, such as in the NR region, the LMPC of Eq. (21) with $O_i = \chi_{p,i}^I$ still yields a unique T_i^* which could characterize the emergence of quantum resonance effects; see Sec. III B and Sec. III C for details.

B. Validity of LMPC for single impurity systems

Before applying the LMPC-based protocol to multi-impurity systems, we first examine its consistency with the MPC-based protocol for single-impurity systems. In principle, the LMPC-based protocol with χ_p^I as the local observable is equivalent to the MPC-based definition with $O = \chi^m$. This is because they both imply

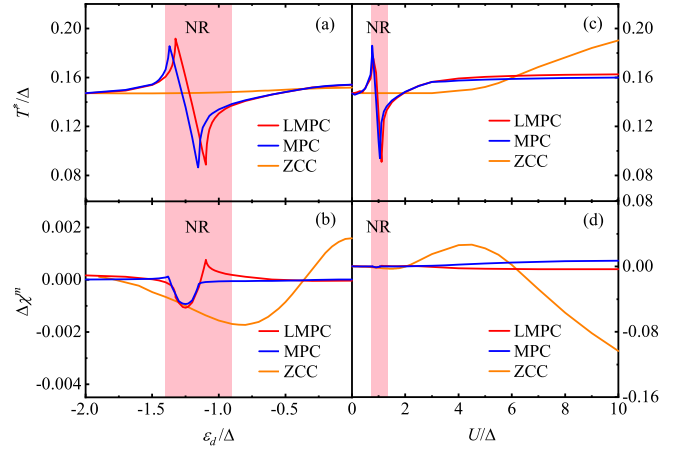


FIG. 4. (a) T^* determined by the ZCC, MPC (with $O = \chi^m$), and LMPC (with $O = \chi_p^I$) as functions of ϵ_d for a noninteracting single-impurity system under an antisymmetric bias voltage of $\mu_R = -\mu_L = V/2 = 0.2\Delta$. (b) The relative deviation from the correspondence relation, $\Delta\chi^m = \chi_{\text{eq}}^m/\chi_{\text{neq}}^m - 1$, versus ϵ_d . (c) T^* determined by the ZCC, MPC, and LMPC as functions of U for an interacting single-impurity system with $\epsilon_d = -2\Delta$ under the same antisymmetric bias voltage. (d) The relative deviation $\Delta\chi^m$ versus U . Other energetic parameters adopted are (in units of Δ): $T_L = T_R = 0.1$, $\Delta_L = \Delta_R = 0.5$, and $W_L = W_R = 20$. The shaded areas represent the NR regions.

the correspondence relation of $\chi_{\text{neq}}^m(T_L, \mu_L, T_R, \mu_R) = \chi_{\text{eq}}^m(T^*, \mu^*, T^*, \mu^*)$, provided that the ZPC for the local observable can be achieved.

Figure 4(a) shows the T^* of a noninteracting single-impurity system under an antisymmetric bias voltage as a function of ϵ_d . It is found that, while the $T^{*,\text{LMPC}}$ agree closely with the $T^{*,\text{MPC}}$ outside the NR region, they display an appreciable difference in the NR region despite the overall similar lineshape.

In the NR region, if the value of the monitored local observable (such as χ_p^I and χ^m) is strongly affected by the emergence of quantum resonances, it could be difficult for O to reach the ZPC by just tuning the T_p . In such a case, the T^* have to be determined by searching for the T_p that yields a minimal nonzero perturbation of O (δO_p). Thus, the resulting $T^{*,\text{LMPC}}$ or $T^{*,\text{MPC}}$ often exhibit a large oscillation because the minimal δO_p tend to vary sensitively due to the nonlocal excitations introduced by the quantum resonances.

Figure 4(b) depicts the relative deviation of χ^m of the nonequilibrium impurity system from that of the reference equilibrium system, $\Delta\chi^m = \chi_{\text{eq}}^m/\chi_{\text{neq}}^m - 1$. Evidently, while $\Delta\chi^m$ almost vanishes with either $T^{*,\text{MPC}}$ or $T^{*,\text{LMPC}}$, it remains of a finite magnitude in the NR region where the ZPC cannot be reached. In contrast, the $T^{*,\text{ZCC}}$ are almost constant in the whole range of ϵ_d with a considerably larger $\Delta\chi^m$, and they show no sign of quantum resonances at all.

Figure 4(c) and (d) depict the T^* and $\Delta\chi^m$ of an in-

interacting single-impurity system under an antisymmetric bias voltage as a function of U , respectively. Similar to the case of a noninteracting impurity, the $T_i^{*,\text{LMPC}}$ and $T_i^{*,\text{MPC}}$ agree closely with each other with a minor difference which is possibly due to the finite band width of the leads. It is worth pointing out that the low background temperature enables the formation of Kondo states,⁸⁰ which provide resonant channels for the electrons to transport across the impurity. Therefore, the system remains in the resonance region with a sufficiently large U ($U > -\epsilon_d$). Again, the $T_i^{*,\text{ZCC}}$ vary rather smoothly and do not reflect the formation of quantum resonant states at all.

The above results verify that the newly proposed LMPC is consistent with the original MPC for single-impurity systems.

C. Local temperatures of multi-impurity systems and the effect of quantum resonances

We now employ the LMPC-based protocol to investigate the distribution of local temperatures in a double-impurity system under an antisymmetric bias voltage. Here, the two impurities are presumed to have the same on-site energy, i.e., $\epsilon_i = \epsilon_d$.

Figure 5 depicts the evolution of (T_i^*, μ_i^*) of the two impurities with the variation of ϵ_d . In analogy with the case of single-impurity systems, while the $T_i^{*,\text{LMPC}}$ agree well with the $T_i^{*,\text{ZCC}}$ in the absence of resonance, they are distinctly different in the two NR regions.

It is worth noting that $T_1^* < T_2^*$ at almost any $\epsilon_d < 0$, which can be explained as follows. With $\epsilon_d < 0$ the total spectral function, $A(\omega)$, of the two impurities has a distribution more on the negative energy side, and this means that the double-impurity system has a positive Seebeck coefficient S .^{76,81} Consequently, the voltage-generated heat current between the two impurities follows the opposite direction of the electric current, i.e., from left to right. Such a heat current thus creates an internal thermal gradient across the two impurities with $T_1^* < T_2^*$.

At $\epsilon_d = 0$, $A(\omega)$ becomes an even function of ω . As a result we have $S = 0$, and hence the voltage-generated internal thermal gradient also becomes zero, i.e., $T_1^* = T_2^*$. This is indeed confirmed by our calculation results shown in Fig. 5(a). Furthermore, it is also inferred that $T_1^* > T_2^*$ at $\epsilon_d > 0$ (data not shown).

It is also interesting to observe that, while the left (right) lead has a lower (higher) chemical potential, the μ_i^* of the neighboring impurity is not necessarily lower (higher); see Fig. 5(b). The fluctuation of μ_i^* manifests the quantum coherence nature of the electron transport driven by the bias voltage. In particular, $\mu_1^* = \mu_2^* = 0$ at $\epsilon_d = -0.9\Delta$, where a resonant state resides right at the center of the nonequilibrium activation window; see the $A(\omega)$ in the inset of Fig. 5(b). The uniformity of μ_i^* indicates that the voltage-driven excitations are pre-

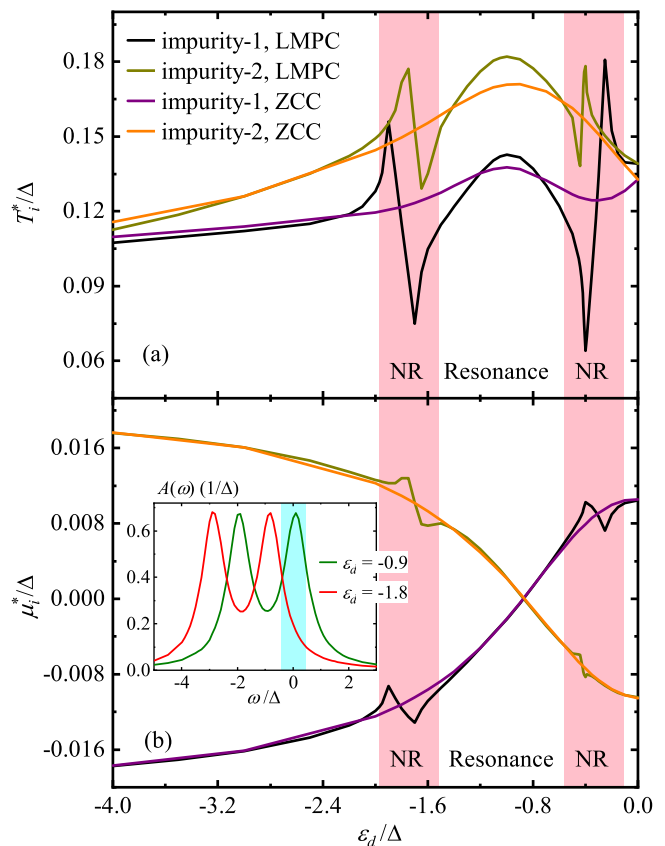


FIG. 5. Evolution of (a) T_i^* and (b) μ_i^* determined by the ZCC and the LMPC with the variation of $\epsilon_i = \epsilon_d$ for a noninteracting double-impurity system under an antisymmetric bias voltage of $\mu_R = -\mu_L = V/2 = 0.2\Delta$. Other energetic parameters adopted are (in units of Δ): $T_L = T_R = 0.1$, $U = 0$, $t = 1$, $\Delta_L = \Delta_R = 0.5$, and $W_L = W_R = 20$. The shaded areas in the main panels represent the NR regions. The inset of (b) depicts the total spectral function of the two impurities $A(\omega)$ at different ϵ_d , where the shaded area indicates the nonequilibrium activation window.

dominantly nonlocal as they occur via the resonant state which involves both impurities.

In Fig. 5, it is again apparent that the (T_i^*, μ_i^*) predicted by the ZCC vary smoothly with ϵ_d , and completely neglect the existence of nonlocal excitations; whereas those determined by the LMPC exhibit large oscillations in the NR regions, which clearly accentuates the emergence of a quantum resonance.

We proceed to study a linear chain comprised of four noninteracting impurities subject to a thermal bias, i.e., $T_L < T_R$. The local chemical potential on each impurity μ_i^* is nearly zero due to the absence of bias voltage. Figure 6 depicts the distribution of T_i^* along the chain determined by the ZCC and the LMPC for various values of t and Δ_α ($\alpha = L, R$).

As shown in Fig. 6(a), when the terminal impurities are coupled strongly to the leads, both the ZCC and the LMPC predict the T_i^* vary almost linearly with i , i.e., the

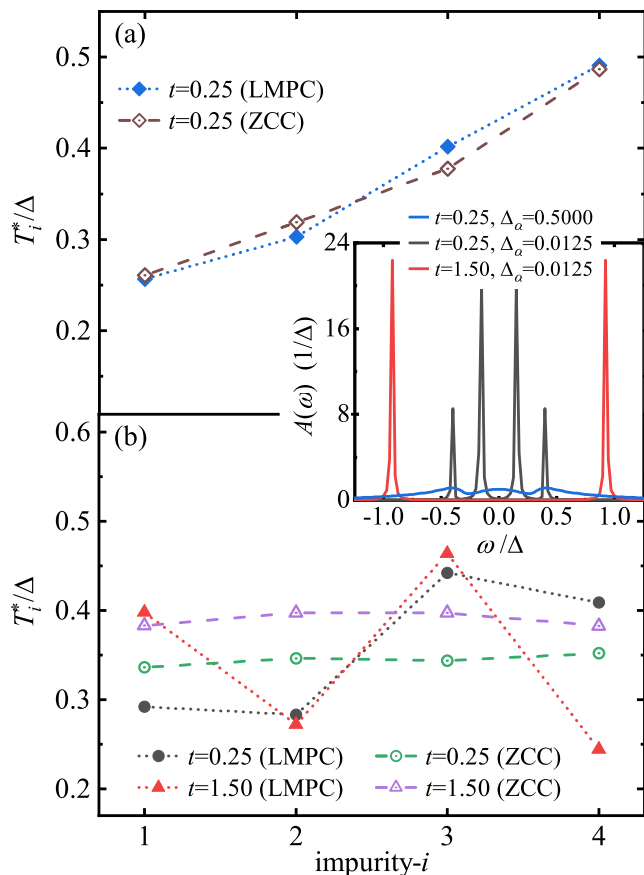


FIG. 6. Local temperature profile T_i^* determined by the ZCC and the LMPC for a noninteracting four-impurity chain under a thermal bias with (a) a strong impurity-lead coupling of $\Delta_\alpha = 0.5\Delta$ ($\alpha = L, R$) and (b) a weak impurity-lead coupling of $\Delta_\alpha = 0.0125\Delta$. Other energetic parameters adopted are (in units of Δ): $\epsilon_i = \epsilon_d = 0$, $U = 0$, $\mu_L = \mu_R = 0$, $T_L = 0.25$, $T_R = 0.5$, $W_L = W_R = 5$. The inset depicts the system spectral function $A(\omega)$ at different t and Δ_α .

distribution of local temperature along the chain obeys the classical Fourier's law.¹ Note that here the restoration of the Fourier's law is not because of disorder⁸² or dephasing caused by an external source,⁸³ which are absent from the AIM under study. Instead, the linear profile of T_i^* is associated with the substantial broadening of the spectral peaks in $A(\omega)$.⁵ This means that the thermal transport process involves electronic states in a wide range of energies. The phases of these states are averaged out when T_i^* are measured, which leads to a classical-like behavior. As the inset of Fig. 6 shows, the impurity-lead coupling Δ_α ($\alpha = L$ or R) affects significantly the sharpness of the peaks, while the coupling strength t between two adjacent impurities has important influence on the distance of neighbouring peaks in a system.

In contrast, Fig. 6(b) concerns another scenario in which the impurity-lead coupling is extremely weak, so that the thermal transport occurs almost exclusively via the quantum resonant states formed on the chain. In

such a scenario, the ZCC and the LMPC yield very different predictions on the distribution of T_i^* . Specifically, the $T_i^{*,ZCC}$ of all the four impurities are close to a certain value between T_L and T_R , while the $T_i^{*,LMPC}$ exhibit large oscillations along the chain, which clearly violates the Fourier's law.

Inui *et al.*⁵ have reported strong oscillations of temperature distribution in a graphene flake weakly coupled to the electrodes under a thermal bias due to quantum interference. But in their study the local temperatures $T_i^{*,ZCC}$ still remain constant on a relatively small scale in the weak-coupling regime, similar to the curve of $T_i^{*,ZCC}$ in Fig. 6(b). Note that the chain in our work is very short, so that even with weak impurity-lead couplings the ZCC-defined T_i^* cannot reveal prominent oscillations. In contrast, the LMPC-defined $T_i^{*,LMPC}$ oscillations in our work are much more significant. In the strong-coupling regime, the temperature profile for the graphene flake is much closer to that predicted by classical Fourier's law,⁵ which is consistent with our results in Fig. 6(a).

IV. CONCLUDING REMARKS

In conclusion, our study of the single-impurity system shows that the MPC predicts a unique local temperature T^* for a given local observable \hat{O} . The value of T^* may be affected by the choice of local observable in the near-resonance (NR) region, where local and nonlocal excitations could both take place inside an impurity system. It is noticed that the MPC-defined T^* deviates from the that determined by the ZCC, although they reach a good agreement outside the NR region. Such a difference indicates that when quantum resonance effects are strong, local temperatures based on different definitions may differ distinctly from one another.

Moreover, we have proposed the protocol of LMPC, by extending the concept of MPC to multi-impurity systems. The LMPC satisfies a correspondence relation, which relates the physical properties of a nonequilibrium system to that of an equilibrium system. Using the LMPC, we studied the effect of quantum resonances on local temperatures of multi-impurity systems. We found that the $T_i^{*,LMPC}$ of double-impurity systems under an antisymmetric bias voltage agree well with the $T_i^{*,ZCC}$ in the absence of resonances. On the other hand, they are distinctly different in the two NR regions, which is analogous to the case of single-impurity systems. Applying the LMPC to a linear chain of four-impurities, we found that the strong quantum resonance effects can lead to prominent local temperature oscillations, which can not be observed by using the ZCC protocol.

By means of the LMPC, some other interesting phenomena in multi-impurity systems may be looked into, such as Peltier cooling, which remains to be further investigated.

ACKNOWLEDGMENTS

The authors acknowledge the support from the Ministry of Science and Technology of China (Grant Nos. 2016YFA0400900, 2016YFA0200600 and 2017YFA0204904), the National Natural Science

Foundation of China (Grant Nos. 21973086 and 21633006), and the Ministry of Education of China (111 Project Grant No. B18051). The computational resources are provided by the Supercomputing Center of University of Science and Technology of China.

-
- * xz58@ustc.edu.cn
 † diventra@physics.ucsd.edu
- ¹ D. Zhang, X. Zheng, and M. Di Ventra, *Phys. Rep.* **830**, 1 (2019).
 - ² E. A. Hoffmann, H. A. Nilsson, J. E. Matthews, N. Nakpathomkun, A. I. Persson, L. Samuelson, and H. Linke, *Nano Lett.* **9**, 779 (2009).
 - ³ F. Menges, H. Riel, A. Stemmer, C. Dimitrakopoulos, and B. Gotsmann, *Phys. Rev. Lett.* **111**, 205901 (2013).
 - ⁴ F. Menges, P. Mensch, H. Schmid, H. Riel, A. Stemmer, and B. Gotsmann, *Nat. Commun.* **7**, 10874 (2016).
 - ⁵ S. Inui, C. A. Stafford, and J. P. Bergfield, *ACS Nano* **12**, 4304 (2018).
 - ⁶ W. Lee, K. Kim, W. Jeong, L. A. Zotti, F. Pauly, J. C. Cuevas, and P. Reddy, *Nature (London)* **498**, 209 (2013).
 - ⁷ L. Cui, R. Miao, K. Wang, D. Thompson, L. A. Zotti, J. C. Cuevas, E. Meyhofer, and P. Reddy, *Nat. Nanotechnol.* **13**, 122 (2018).
 - ⁸ D. Novko, J. C. Tremblay, M. Alducin, and J. I. Juaristi, *Phys. Rev. Lett.* **122**, 016806 (2019).
 - ⁹ M. P. Zeidler, C. Tan, Y. Bellaiche, S. Cherry, S. Häder, U. Gayko, and N. Perrimon, *Nat. Biotechnol.* **22**, 871 (2004).
 - ¹⁰ G. Kucsko, P. C. Maurer, N. Y. Yao, M. Kubo, H. J. Noh, P. K. Lo, H. Park, and M. D. Lukin, *Nature (London)* **500**, 54 (2013).
 - ¹¹ Y.-M. He and B.-G. Ma, *Sci. Rep.* **6**, 26737 (2016).
 - ¹² S. Sadat, E. Meyhofer, and P. Reddy, *Rev. Sci. Instrum.* **83**, 084902 (2012).
 - ¹³ M. Mecklenburg, W. A. Hubbard, E. R. White, R. Dhall, S. B. Cronin, S. Aloni, and B. C. Regan, *Science* **347**, 629 (2015).
 - ¹⁴ K. L. Grosse, M.-H. Bae, F. Lian, E. Pop, and W. P. King, *Nat. Nanotechnol.* **6**, 287 (2011).
 - ¹⁵ S. P. Gurrum, Y. K. Joshi, W. P. King, and K. Ramakrishna, *J. Heat Transfer*. **127**, 809 (2005).
 - ¹⁶ M. Di Ventra, *Electrical Transport in Nanoscale Systems*, Cambridge University Press, Cambridge, 2008.
 - ¹⁷ S. Liu, A. Nurbawono, and C. Zhang, *Sci. Rep.* **5**, 15386 (2015).
 - ¹⁸ Z. Huang, B. Xu, Y. Chen, M. Di Ventra, and N. Tao, *Nano Lett.* **6**, 1240 (2006).
 - ¹⁹ Z. Huang, F. Chen, R. D'agosta, P. A. Bennett, M. Di Ventra, and N. Tao, *Nat. Nanotechnol.* **2**, 698 (2007).
 - ²⁰ K. Kim, W. Jeong, W. Lee, S. Sadat, D. Thompson, E. Meyhofer, and P. Reddy, *Appl. Phys. Lett.* **105**, 203107 (2014).
 - ²¹ H. Thierschmann, R. Sánchez, B. Sothmann, F. Arnold, C. Heyn, W. Hansen, H. Buhmann, and L. W. Molenkamp, *Nat. Nanotechnol.* **10**, 854 (2015).
 - ²² I. Lončarić, M. Alducin, P. Saalfrank, and J. I. Juaristi, *Phys. Rev. B* **93**, 014301 (2016).
 - ²³ J. C. Idrobo, A. R. Lupini, T. Feng, R. R. Unocic, F. S. Walden, D. S. Gardiner, T. C. Lovejoy, N. Dellby, S. T. Pantelides, and O. L. Krivanek, *Phys. Rev. Lett.* **120**, 095901 (2018).
 - ²⁴ H. E. D. Scovil and E. O. Schulz-DuBois, *Phys. Rev. Lett.* **2**, 262 (1959).
 - ²⁵ F. L. Curzon and B. Ahlborn, *Am. J. Phys.* **43**, 22 (1975).
 - ²⁶ E. H. Lieb and J. Yngvason, *Phys. Rep.* **310**, 1 (1999).
 - ²⁷ A. E. Allahverdyan and T. M. Nieuwenhuizen, *Phys. Rev. E* **64**, 056117 (2001).
 - ²⁸ J. Casas-Vázquez and D. Jou, *Rep. Prog. Phys.* **66**, 1937 (2003).
 - ²⁹ T. D. Kieu, *Phys. Rev. Lett.* **93**, 140403 (2004).
 - ³⁰ C. Bustamante, J. Liphardt, and F. Ritort, *Phys. Today* **58**, 43 (2005).
 - ³¹ C. Hörhammer and H. Büttner, *J. Stat. Phys.* **133**, 1161 (2008).
 - ³² J. P. Bergfield and C. A. Stafford, *Phys. Rev. B* **79**, 245125 (2009).
 - ³³ A. Levy, R. Alicki, and R. Kosloff, *Phys. Rev. E* **85**, 061126 (2012).
 - ³⁴ M. Horodecki and J. Oppenheim, *Nat. Commun.* **4**, 2059 (2013).
 - ³⁵ P. Skrzypczyk, A. J. Short, and S. Popescu, *Nat. Commun.* **5**, 4185 (2014).
 - ³⁶ A. Ü. C. Hardal and Ö. E. Müstecaplıoğlu, *Sci. Rep.* **5**, 12953 (2015).
 - ³⁷ G. Clos, D. Porras, U. Warring, and T. Schaetz, *Phys. Rev. Lett.* **117**, 170401 (2016).
 - ³⁸ A. Puglisi, A. Sarracino, and A. Vulpiani, *Phys. Rep.* **709**, 1 (2017).
 - ³⁹ S. Marcantoni, S. Alipour, F. Benatti, R. Floreanini, and A. T. Rezakhani, *Sci. Rep.* **7**, 12447 (2017).
 - ⁴⁰ J. Monsel, C. Elouard, and A. Auffèves, *npj Quantum Inf.* **4**, 59 (2018).
 - ⁴¹ P. Bialas, J. Spiechowicz, and J. Luczka, *J. Phys. A: Math. Theor.* **52**, 15LT01 (2019).
 - ⁴² H.-L. Engquist and P. W. Anderson, *Phys. Rev. B* **24**, 1151 (1981).
 - ⁴³ J. Meair, J. P. Bergfield, C. A. Stafford, and P. Jacquod, *Phys. Rev. B* **90**, 035407 (2014).
 - ⁴⁴ J. P. Bergfield and C. A. Stafford, *Phys. Rev. B* **90**, 235438 (2014).
 - ⁴⁵ A. Shastry and C. A. Stafford, *Phys. Rev. B* **92**, 245417 (2015).
 - ⁴⁶ C. A. Stafford, *Phys. Rev. B* **93**, 245403 (2016).
 - ⁴⁷ C. A. Stafford and A. Shastry, *J. Chem. Phys.* **146**, 092324 (2017).
 - ⁴⁸ K. H. Bevan, *Nanotechnology* **25**, 415701 (2014).
 - ⁴⁹ D. K. Morr, *Contemp. Phys.* **57**, 19 (2016).
 - ⁵⁰ D. K. Morr, *Phys. Rev. B* **95**, 195162 (2017).
 - ⁵¹ A. Caso, L. Arrachea, and G. S. Lozano, *Phys. Rev. B* **81**, 041301(R) (2010).

- ⁵² A. Caso, L. Arrachea, and G. S. Lozano, *Phys. Rev. B* **83**, 165419 (2011).
- ⁵³ A. Caso, L. Arrachea, and G. S. Lozano, *Eur. Phys. J. B* **85**, 266 (2012).
- ⁵⁴ Y. Dubi and M. Di Ventra, *Nano Lett.* **9**, 97 (2009).
- ⁵⁵ M. Michel, M. Hartmann, J. Gemmer, and G. Mahler, *Eur. Phys. J. B* **34**, 325 (2003).
- ⁵⁶ A. Dhar, *Adv. Phys.* **57**, 457 (2008).
- ⁵⁷ D. Roy, *Phys. Rev. E* **77**, 062102 (2008).
- ⁵⁸ N. Yang, G. Zhang, and B. Li, *Nano Today* **5**, 85 (2010).
- ⁵⁹ J. P. Bergfield, S. M. Story, R. C. Stafford, and C. A. Stafford, *ACS Nano* **7**, 4429 (2013).
- ⁶⁰ J. P. Bergfield, M. A. Ratner, C. A. Stafford, and M. Di Ventra, *Phys. Rev. B* **91**, 125407 (2015).
- ⁶¹ A. Shastry and C. A. Stafford, *Phys. Rev. B* **94**, 155433 (2016).
- ⁶² L. Z. Ye, X. Zheng, Y. J. Yan, and M. Di Ventra, *Phys. Rev. B* **94**, 245105 (2016).
- ⁶³ L. Z. Ye, D. Hou, X. Zheng, Y. J. Yan, and M. Di Ventra, *Phys. Rev. B* **91**, 205106 (2015).
- ⁶⁴ P. W. Anderson, *Phys. Rev.* **124**, 41 (1961).
- ⁶⁵ Y. Tanimura and R. Kubo, *J. Phys. Soc. Jpn.* **58**, 101 (1989).
- ⁶⁶ J. Jin, X. Zheng, and Y. J. Yan, *J. Chem. Phys.* **128**, 234703 (2008).
- ⁶⁷ Z. H. Li, N. H. Tong, X. Zheng, D. Hou, J. H. Wei, J. Hu, and Y. J. Yan, *Phys. Rev. Lett.* **109**, 266403 (2012).
- ⁶⁸ L. Cui, H.-D. Zhang, X. Zheng, R.-X. Xu, and Y. J. Yan, *J. Chem. Phys.* **151**, 024110 (2019).
- ⁶⁹ H.-D. Zhang, L. Cui, H. Gong, R.-X. Xu, X. Zheng, and Y. J. Yan, *J. Chem. Phys.* **152**, 064107 (2020).
- ⁷⁰ Y. Tanimura, *J. Chem. Phys.* **153**, 020901 (2020).
- ⁷¹ L. Z. Ye, X. Wang, D. Hou, R.-X. Xu, X. Zheng, and Y. J. Yan, *WIREs Comput. Mol. Sci.* **6**, 608 (2016).
- ⁷² L. Han, H.-D. Zhang, X. Zheng, and Y. J. Yan, *J. Chem. Phys.* **148**, 234108 (2018).
- ⁷³ X. Zheng, J. Jin, S. Welack, M. Luo, and Y. J. Yan, *J. Chem. Phys.* **130**, 164708 (2009).
- ⁷⁴ X. Zheng, Y. J. Yan, and M. Di Ventra, *Phys. Rev. Lett.* **111**, 086601 (2013).
- ⁷⁵ S. Wang, X. Zheng, J. Jin, and Y. J. Yan, *Phys. Rev. B* **88**, 035129 (2013).
- ⁷⁶ L. Z. Ye, D. Hou, R. Wang, D. Cao, X. Zheng, and Y. J. Yan, *Phys. Rev. B* **90**, 165116 (2014).
- ⁷⁷ D. Hou, S. Wang, R. Wang, L. Z. Ye, R.-X. Xu, X. Zheng, and Y. J. Yan, *J. Chem. Phys.* **142**, 104112 (2015).
- ⁷⁸ X. Wang, L. Yang, L. Z. Ye, X. Zheng, and Y. J. Yan, *J. Phys. Chem. Lett.* **9**, 2418 (2018).
- ⁷⁹ X. Li, L. Zhu, B. Li, J. Li, P. Gao, L. Yang, A. Zhao, Y. Luo, J. Hou, X. Zheng, B. Wang, and J. Yang, *Nat. Commun.* **11**, 2566 (2020).
- ⁸⁰ Y. Meir, N. S. Wingreen, and P. A. Lee, *Phys. Rev. Lett.* **70**, 2601 (1993).
- ⁸¹ B. Dong and X. L. Lei, *J. Phys.: Condens. Matter* **14**, 11747 (2002).
- ⁸² Y. Dubi and M. Di Ventra, *Phys. Rev. B* **79**, 115415 (2009).
- ⁸³ Y. Dubi and M. Di Ventra, *Phys. Rev. E* **79**, 042101 (2009).